Responses to the Reviewer

We would like to express our profound gratitude to you for your insightful comments and suggestions. Your expertise has significantly contributed to the enhancement of our study. In response to your valuable feedback, we have made corresponding revisions and additions to the manuscript. The detailed responses to each point raised are presented in the following sections. The responses are highlighted in blue, and the changes made in the manuscript are marked in red. We sincerely hope that these revisions adequately address your concerns.

General Comments:

This study estimated the aerodynamic roughness length (z_0) values using ERA5 analyses and weather station observations to improve the near-surface wind speed modeling. Technically, the Random Forest Regression algorithm is suitable for the estimation of z_0, and the results are encouraging, significantly improving the wind speed simulation in the WRF model. However, the evaluation of the improved z_0 on the WRF near-surface wind simulation was only for one month, and a longer time evaluation is needed. Therefore, I recommend Major Revision in this round.

Response: We are sincerely grateful for your positive feedback and constructive comments. Your comments have been thoroughly considered and have greatly contributed to the improvement of our manuscript. Our point-by-point responses are detailed below.

Specific comments:

Major comments:

1. The new estimated z_0 values were only evaluated for 1 month. A longer time evaluation should be conducted for a thorough evaluation.

Response: Thank you for your insightful comment. In our study, we initially evaluated the performance of the newly estimated aerodynamic roughness length (z_0) using wind simulations for the month of April in 2019. April was deliberately chosen as the primary evaluation period because it exhibits the highest mean wind speeds across our study domain (Fig. R1), making the simulated wind fields particularly sensitive to z_0 effects. This characteristic provides an ideal scenario for testing the impact and effectiveness of our proposed estimation method. To balance computational cost with scientific rigor, we implemented a re-initialization strategy whereby each 36-hour simulation was initialized daily at 12:00 LT (LT = UTC+8). Each simulation included a 12-hour spin-up period followed by 24 hours of analysis, yielding 30 independent realizations. This approach ensured the capture of a wide range of meteorological conditions while maintaining statistical independence among daily cases. As presented in Section 3.3, the consistent improvement in simulated wind speeds across all April cases demonstrates the robustness of the newly estimated z_0.

To address the concern regarding longer-term evaluation, we additionally conducted WRF simulations for October 2019, a month characterized by generally weaker wind conditions (Fig. R1), using the same model configuration and evaluation framework as applied for April. The results from these additional simulations (Figs. R2-R4) further confirm the robustness of our method, as the use of the newly estimated z_0 values consistently improves the accuracy of simulated wind speeds.

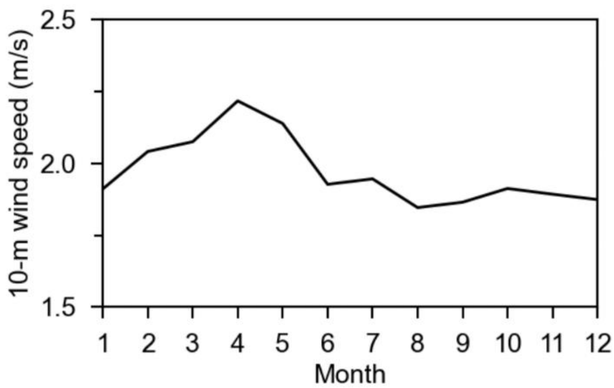

Figure R1 (**Figure S3 in the Supplement**). Monthly variations of the 10-m wind speed averaged over the d02 domain during 2015-2019 from ERA5.

The results of these additional simulations have been included in the Supplement (Figs. S5-S7), and a corresponding explanation has been incorporated into the revised manuscript in lines 332-338, replacing the original sentence: "In summary, the z_0 derived from the combination of CMA and ERA5 data shows high reliability, and the resulting gridded z_0 dataset in built-up areas can effectively reduce uncertainties in mesoscale near-surface wind speed simulations, especially over relatively flat built-up regions." with the following revised version: "In summary, the 30 independent simulation cases conducted for April demonstrate that the z_0 values derived from the combination of CMA observations and ERA5 data are highly reliable. The resulting gridded z_0 dataset significantly reduces uncertainties in mesoscale near-surface wind speed simulations, particularly over relatively flat built-up areas. To further validate the robustness of the z_0 estimation method and the resulting dataset, we conducted additional simulations for October 2019, a month characterized by generally weaker wind conditions (Fig. S3), using the same model configuration as in April. The results (Figs. S5-S7) also show consistent improvements when using z_{0_RFR}, further reinforcing the reliability and applicability of the proposed z_0 estimation approach under varying meteorological conditions."

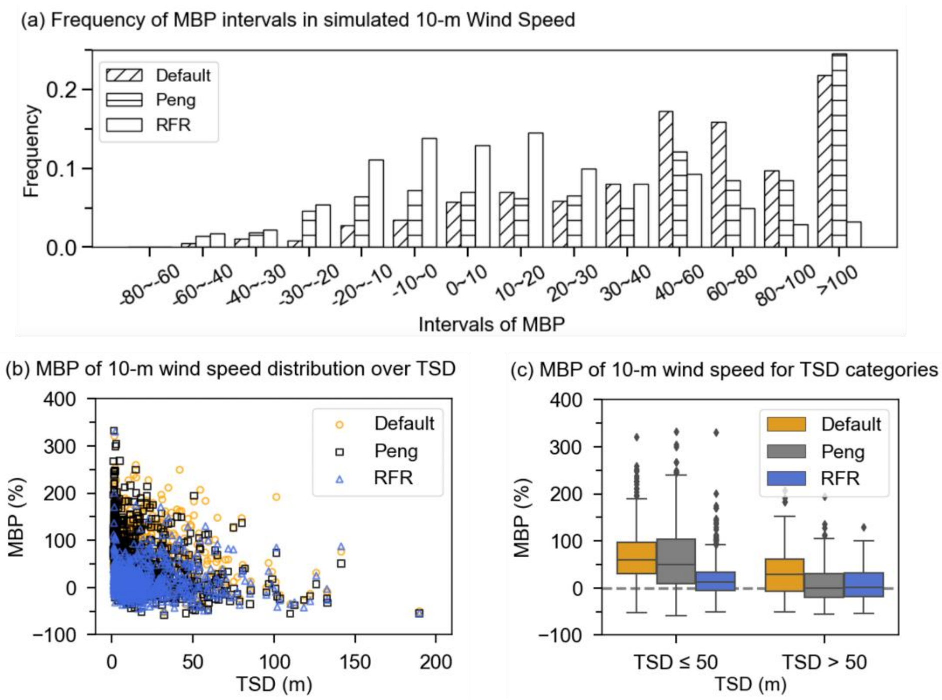

Figure R2 (Figure S5 in the Supplement). (a) Frequency distribution of *MBP* in simulated 10-m wind speed in October using $z_{0\_Default}$, z_{0_Peng}, and z_{0_RFR} against observations from CMA stations. *MBP* was calculated as $[u_{simulations} - u_{CMA}]/u_{CMA} \times 100\%$. (b) Distribution of *MBP* in 10-m wind speed as a function of *TSD*. (c) Box plot of *MBP* in 10-m wind speed across different *TSD* bins.

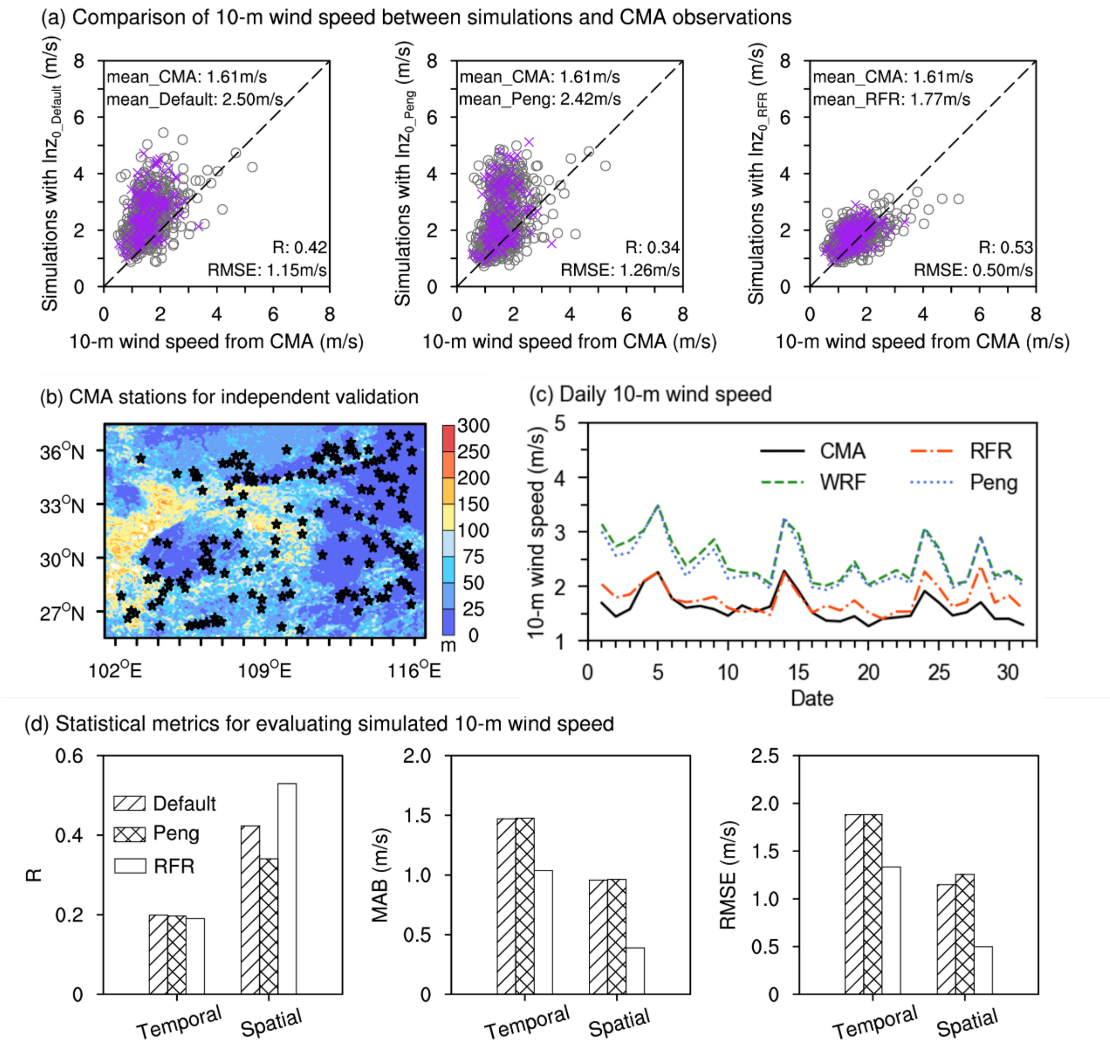

Figure R3 (**Figure S6 in the Supplement**). (a) Comparisons of mean 10-m wind speed in October between the simulations using $z_{0\_Default}$, z_{0_Peng}, and z_{0_RFR} versus observations from CMA stations. All points (grey circles and purple crosses) represent the 753 CMA stations within the d02 domain available for comparison, while the purple crosses represent the 155 stations utilized for independent validation, which were not used in training the z_{0_RFR} model. The corresponding wind speed means, correlation coefficients (*R*), and root mean square errors (*RMSE*) of all stations are also indicated. (b) Distribution of the 155 independent CMA stations (black stars). Colored shaded areas represent *TSD*. (c) Comparison of daily mean 10-m wind speed between simulations and observations from 753 CMA stations. (d) Statistical metrics comparing simulated and observed 10-m wind speeds, including temporal and spatial *R*, mean absolute bias (*MAB*, $\frac{1}{N}\sum_{i=1}^{N}\left|u_i^{simulation} - u_i^{observation}\right|$, where N represents the number of hours for temporal *MAB*, and the number of stations for spatial *MAB*) and *RMSE*.

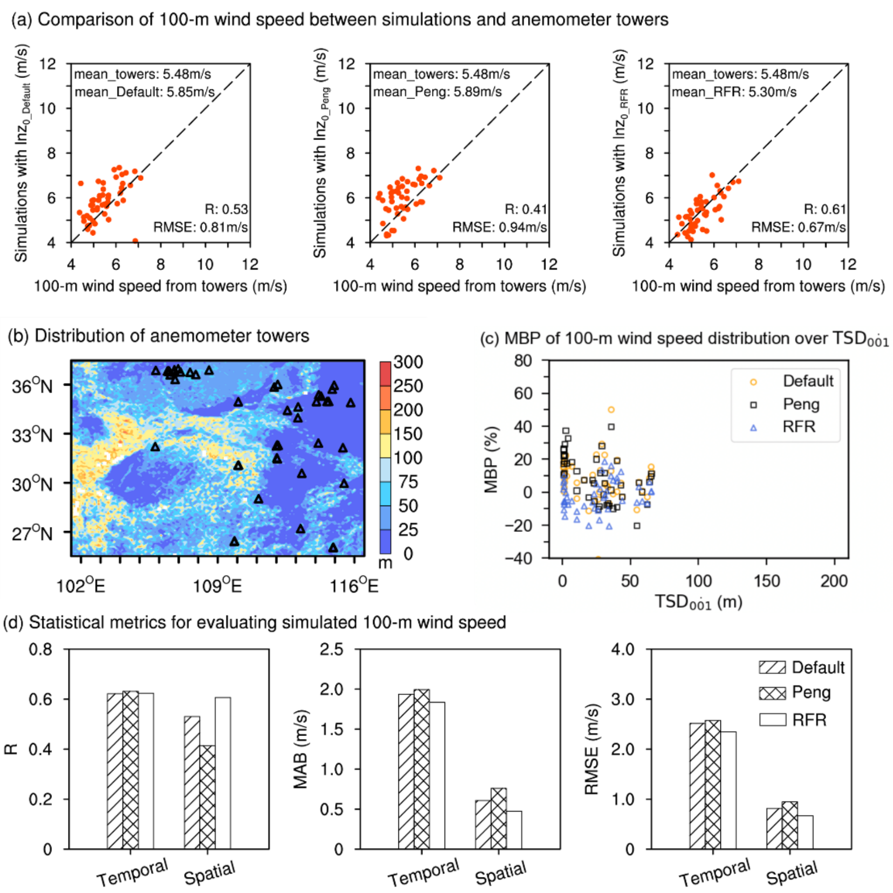

Figure R4 (**Figure S7 in the Supplement**). (a) Comparisons of mean 100-m wind speed in October between the simulations using $z_{0\_Default}$, z_{0_Peng}, and z_{0_RFR} versus observations from anemometer towers. The corresponding wind speed means, *R*, and *RMSE* of all towers are also indicated. (b) The locations of 48 anemometer towers (black triangles) utilized for 100-m wind speed evaluation. Colored shaded areas represent *TSD*. (c) Distribution of *MBP* in 100-m wind speed as a function of *TSD*. *MBP* was calculated as $[u_{simulations} - u_{towers}]/u_{towers} \times 100\%$. (d) Statistical metrics comparing simulated and observed 100-m wind speeds, including temporal and spatial *R*, *MAB*, and *RMSE*.

2. The grid-based z_0 statistics are only available in the inner domain. This indicates that the z_0 could only be improved where there are surface weather station observations. How to improve the z_0 destination in areas where there is no good coverage of surface weather station observations? More discussions should be included.

Response: We greatly appreciate your valuable question. We agree that the current implementation of our method is limited by the availability of surface weather station observations, which poses a challenge for estimating z_0 in areas with sparse or no such coverage. Nevertheless, these under-observed regions, such as northern and northwestern China, are key zones for wind energy development. Thus, producing high-quality gridded z_0 datasets in these areas is not only of scientific interest but also crucial for enhancing the accuracy of wind speed simulations in practical applications.

A sufficient number of z_0 truth values is essential for generating such gridded datasets. The lack of z_0 truth values in station-sparse regions remains a major barrier. With the rapid growth of the wind energy industry, tens of thousands of such towers have been deployed for wind resource assessments. This development may offer a valuable opportunity to expand z_0 truth values and to construct a gridded z_0 dataset once these tower data are accessible.

We have included a discussion on this point in Section "4 Discussion" of the revised manuscript (lines 371-375), where we state: "However, this method is limited in regions with sparse or no surface weather stations. Notably, these regions, such as western and northern China, are rich in wind resources and are key targets for wind energy development. Therefore, producing high-quality gridded z_0 datasets in these regions warrants further study by exploring alternative data sources, such as anemometer tower wind profiles, to supplement z_0 truth values (Wang et al., 2024)."

Minor comments:

1. Line 39-41: It is a little bit causing here. Please revise it to be more clear.

Response: Thank you for your constructive reminder. We have revised "The utilization of wind energy in built-up areas also depends on wind speed distribution (Ishugah et al., 2014; Stathopoulos et al., 2018; Tasneem et al., 2020). Whether establishing wind farms in urban suburbs or integrating wind turbines into building designs, both can help to reduce generation load and the need for transmission infrastructure. Additionally, wind speed profoundly affects building design and urban planning (Hadavi and Pasdarshahri, 2020) and even the preservation of historical-cultural heritage (Li, Y. et al., 2023)." into "The utilization of wind energy in built-up areas also depends on wind speed distribution (Ishugah et al., 2014; Stathopoulos et al., 2018; Tasneem et al., 2020).

Proper utilization, through measures such as suburban wind farms or building-integrated turbines, can minimize the need for transmission infrastructure. Beyond energy considerations, wind speed characteristics play a critical role in urban design and planning, influencing both contemporary building practices (Hadavi and Pasdarshahri, 2020) and the preservation of historical-cultural heritage (Li, Y. et al., 2023)." in lines 37-42 of the revised manuscript.

2. Line 47: ERA5 is the analysis from a DA system. In my opinion, it is the blend of observations and model forecasts. Therefore, it is not proper to use it as an example.

Response: Thank you for your comment. We fully acknowledge that ERA5 is a reanalysis dataset generated through a data assimilation (DA) system, produced using 4D-Var DA and model forecasts in CY41R2 of the ECMWF Integrated Forecast System (IFS). However, it is important to note that the assimilated observations, especially over regions such as China, are relatively limited in spatial coverage. This partly explains the poor performance of ERA5 in representing wind speeds near the surface. Wang et al. (2024) evaluated the performance of ERA5 10-m wind speeds in China using data from both surface weather stations and anemometer towers, and found significant biases (Fig. R5). These biases indicate that the representation of near-surface wind conditions in ERA5 still heavily relies on the underlying model parameterizations, including the use of fixed z_0 based on land cover types. Therefore, we believe that using ERA5 as an example remains appropriate in the context of illustrating the limitations of z_0 treatment in current model frameworks.

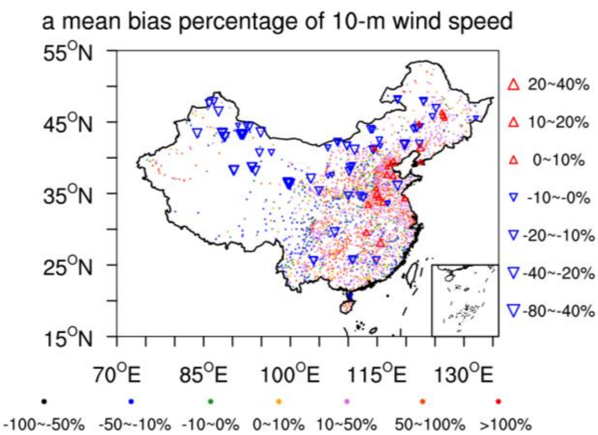

Figure R5 (**Figure 4a from Wang et al. (2024)**). The distribution of MBP of 10-m wind speed between ERA5 and measurements ($(ERA5 - measurements)/measurements \times 100\%$). The dots and triangles represent the measurements from CMA stations and anemometer towers.

3. Line 54: What does it mean here "low-type" and "high-type"?

Response: Thank you for your insightful question. In this context, "low-type" and "high-type" vegetation refer to categories based on vegetation height. Specifically, "low-type" vegetation typically includes shorter land cover types such as grasslands and croplands, while "high-type" vegetation refers to taller vegetation such as forests. To enhance clarity, we have revised the sentence as follows: "In line with these findings, Luu et al. (2023) showed that the rise in z_0, caused by shifts from short vegetation to high vegetation and urbanization, partly contributes to the decline in mean and maximum surface wind speed over Western Europe." in lines 53-55 of the revised manuscript.

4. Line 87: Better to add surface weather station observations before CMA.

Response: Thank you for your useful suggestion. We have added "surface weather station observations" before "CMA" in lines 87-88 of the revised manuscript.

5. Line 192: This could be because of the altitude differences between observation sites and the model terrain.

Response: Thank you for your insightful comment. The altitude differences between observation sites and the model terrain could indeed contribute to the poor performance of ERA5 100-m wind speed data in these areas. To reflect this, we have revised the sentence as follows: "The exclusions of these stations can be attributed to the poor performance of ERA5 100-m wind speed data, which may result from altitude differences between the observation sites and the model terrain, thereby rendering our initial assumption, i.e. ERA5 100-m wind speed data are reliable for z_0 estimation, invalid in these areas." in lines 192-195 of the revised manuscript.

6. Line 227: What is the temporal coverage of this monthly z_0 dataset?

Response: Thank you for your insightful question. In this study, our primary objective was to propose a cost-effective method for estimating z_0 using weather station observations and reanalysis data. Accordingly, the monthly gridded z_0 dataset we produced, referred to as z_{0_RFR}, was mainly intended to demonstrate the feasibility and effectiveness of the z_0 estimation approach through wind speed simulations. For this purpose, the z_{0_RFR} dataset was generated for the year 2019 as a representative example. It is important to note, however, that the Random Forest Regression (RFR) model developed for generating the gridded z_{0_RFR} dataset is not limited to a specific year. It can readily be applied to other years, provided that the corresponding input features are available.

To clarify this point, we have revised the manuscript and added the following statements: "As a representative example, the z_{0_RFR} dataset was generated for the year 2019, and its spatial coverage is shown in Fig. 2d." (lines 231-232) and "Although 2019 was chosen for demonstration, the RFR model itself is year-independent and can be applied to other years, provided that the required input features are available." (lines 235-237).

7. Figure 5: better to a reference line of y = 0 in panel (c) for reference, indicating which has a smaller bias.

Response: Thank you for your constructive suggestion. We have added a reference line at $y = 0$ in Fig. 5c to indicate the direction and magnitude of the bias more clearly.

8. Line 317: The values are significantly large when verified against the Mean values. However, if you take a deep look at Fig. 7d, the improvements are not that large from the perspective of MAB and RMSE.

Response: Thank you for your insightful comment. In line 317 of the original manuscript, we stated: "This improvement using z_{0_RFR} reduces wind speed mean bias by 85.7% and 88.1% compared to $z_{0\_Default}$ and z_{0_Peng}, respectively.", which indeed shows a substantial improvement. While this appears to contrast with the results presented in Fig. 7d, where the reductions in *MAB* and *RMSE* seem less pronounced, this discrepancy arises from the use of different evaluation metrics. Specifically, the percentage reduction of wind speed mean bias refers to the relative decrease in mean error. For example, in the simulation based on $z_{0\_Default}$ the average 100-m wind speed is 7.10 m/s; while using z_{0_RFR}, it is 6.38 m/s. The corresponding observed value from the anemometer towers is 6.26 m/s. Thus, the mean bias is reduced from 0.84 m/s $(7.10 - 6.26)$ to 0.12 m/s $(6.38 - 6.26)$, leading to a bias reduction of $(0.84 - 0.12) \div 0.84 \times 100\% = 85.7\%$.

In addition, even when evaluated using the *MAB* and *RMSE* metrics shown in Fig. 7d, the improvements brought by z_{0_RFR} are still considerable. Specifically, in the spatial dimension, the 100-m wind speed simulations based on $z_{0\_Default}$ and z_{0_Peng} show *MAB* values of 1.12 m/s and 1.47 m/s, respectively, while the simulation using z_{0_RFR} yields a significantly lower *MAB* of 0.58 m/s. Similarly, the corresponding *RMSE* values are 1.31 m/s for $z_{0\_Default}$, 1.63 m/s for z_{0_Peng}, and 0.82 m/s for z_{0_RFR}. Although the improvements in the temporal dimension are not as pronounced as those in the spatial dimension, they are still evident. These results further confirm the overall improvement achieved by incorporating the z_{0_RFR}.

To enhance clarity, we have added the formula used to calculate the percentage reduction in wind speed mean bias to the revised manuscript, as shown in the caption of Table 1: "The percentage reduction in wind speed error is caused by z_{0_RFR}, compared to $z_{0\_Default}$ and z_{0_Peng}, which is calculated as $\left[\left|\bar{u}_{z_{0\_*}} - \bar{u}_{observation}\right| - \left|\bar{u}_{z_{0\_RFR}} - \bar{u}_{observation}\right|\right] / \left|\bar{u}_{z_{0\_*}} - \bar{u}_{observation}\right| \times 100\%$, where $\bar{u}_{z_{0\_*}}$ represents $\bar{u}_{z_{0\_Default}}$ or $\bar{u}_{z_{0\_Peng}}$, and $\bar{u}$ denotes the mean 10-m or 100-m wind speed from simulations based on $z_{0\_Default}$, z_{0_Peng}, and z_{0_RFR}, as well as from observations (CMA stations or anemometer towers)."

9. Figure 7: Better to add statists of mean/rms/r in the panels of (a). For (d), the units of MAB is not m/s, likely %.

Response: Thank you for your suggestion. We have added the statistics of mean, *RMSE*, and correlation coefficient (R) to both Fig. 6a and Fig. 7a in the revised manuscript.

MAB refers to mean absolute bias, which is calculated as $\frac{1}{N}\sum_{i=1}^{N}\left|u_i^{simulation} - u_i^{observation}\right|$, where N represents the number of stations for spatial *MAB*, and the number of hours for temporal *MAB*. Therefore, the unit of *MAB* is m/s.

To enhance clarity, we have included the formula for *MAB* at its first occurrence, in the caption of Fig. 6 in the revised manuscript, as follows: "Figure 6. (a) Comparisons of mean 10-m wind speed in April between the simulations using $z_{0\_Default}$, z_{0_Peng}, and z_{0_RFR} versus observations from CMA stations. All points (grey circles and purple crosses) represent the 753 CMA stations within the d02 domain available for comparison, while the purple crosses represent the 155 stations utilized for independent validation, which were not used in training the z_{0_RFR} model. The corresponding wind speed means, correlation coefficients (*R*), and root mean square errors (*RMSE*) of all stations are also indicated. (b) Distribution of the 155 independent CMA stations (black stars). Colored shaded areas represent *TSD*. (c) Comparison of daily mean 10-m wind speed between simulations and observations from 753 CMA stations. (d) Statistical metrics comparing simulated and observed 10-m wind speeds, including temporal and spatial *R*, mean absolute bias (*MAB*, $\frac{1}{N}\sum_{i=1}^{N}\left|u_i^{simulation} - u_i^{observation}\right|$, where N represents the number of hours for temporal *MAB*, and the number of stations for spatial *MAB*) and *RMSE*."

Reference

Wang, J., Yang, K., Yuan, L., Liu, J., Peng, Z., Ren, Z. and Zhou, X.: Deducing aerodynamic roughness length from abundant anemometer tower data to inform wind resource modeling, Geophys. Res. Lett., 51, e2024GL111056, doi:10.1029/2024GL111056, 2024.